Journal of Alloys and Compounds 619 (2015) 31–37

Contents lists available at ScienceDirect

Journal of Alloys and Compounds

journal homepage: www.elsevier.com/locate/jalcom

Thermoelectric performance of higher manganese silicide nanocomposites

M. Saleemi [a,*], A. Famengo [b], S. Fiameni [b], S. Boldrini [b], S. Battiston [b], M. Johnsson [c], M. Muhammed [a], M.S. Toprak [a,*]

[a] Department of Materials and Nano Physics, KTH Royal Institute of Technology, Kista, Stockholm, Sweden
[b] CNR, Institute for Energetics and Interphases (IENI-CNR), Corso Stati Uniti 4, I-35127 Padua, Italy
[c] Department of Materials and Environmental Chemistry, Stockholm University, Stockholm, Sweden

ARTICLE INFO

Article history:
Received 24 July 2014
Received in revised form 29 August 2014
Accepted 1 September 2014
Available online 16 September 2014

Keywords:
Thermoelectrics
Higher manganese silicide
Spark plasma sintering
Nanostructured

ABSTRACT

Higher manganese silicides (HMS) are proven to be promising candidates as p-type thermoelectric material in the temperature range of 400–700 K. In this work, a series of nanostructured (NS) bulk $MnSi_{1.73}$ with different levels of Ytterbium inclusions were fabricated via ball milling and the solid state reaction was completed by spark plasma sintering (SPS). Nanopowders and SPS consolidated Yb–HMS nanocomposites (NC) were characterized by X-ray diffraction (XRD) and scanning electron microscopy (SEM) to reveal the crystal structure and morphology respectively. High resolution transmission electron microscopy (HRTEM) coupled with energy dispersive X-ray spectroscopy (EDS) was used to investigate the material composition in bulk grains. Yb was observed to stay as nanoinclusions at the grain boundaries. TE transport properties, including Seebeck coefficient, electrical resistivity, and thermal diffusivity as well as charge carrier concentrations were evaluated. Thermal conductivity decreased with increasing Yb content, while the electrical conductivity improved for the highest Yb content. A highest figure of merit (ZT) of 0.42 at 600 °C was achieved for 1% Yb–HMS NC sample.

1. Introduction

High fuel prices and extensive consumption of the fossil fuels are hauling this world through imminent energy crisis. Thermoelectric generators (TEGs) may play a key role to meet this challenge as they can produce electricity from waste heat sources, including cars and various industries [1]. For instance, TEGs in car exhaust pipes with a conversion efficiency of 10–15% will reduce the fuel consumption by around 3–6%, which is potentially significant to meet the 2020 carbon emission goal for the car industry [2]. Thermoelectric (TE) materials are widely explored and their efficiency is defined by the dimensionless figure of merit, $ZT = \frac{S^2}{\rho\kappa}T$, where S is the Seebeck coefficient, ρ is the electrical resistivity, κ is the thermal conductivity, that is the sum of electronic (κ_e) and lattice (κ_l) conductivity contributions and T is the absolute temperature [3]. Acquiring high ZT value is often challenging due to the interdependence of these physical parameters. Many groups reported on the possibility of enhancing power factor (S^2/ρ) and reduced thermal conductivity with multiple nano-engineering approaches [4–9].

TE materials are categorized depending upon their application temperature range; chalcogenides are effective at low temperature (below 250 °C), skutterudites are promising at intermediate temperature (up to 500 °C) [10], and in case of high temperature (more than 600 °C) half-Heusler compounds, and transition metal oxides are representative examples [11]. Although these TE materials showed improved performance, they cannot dominate the TE market because most of their constituents are toxic, less abundant and/or very expensive [12]. This may hinder their further implementation for mass production. Silicide based materials are considered as the best candidate for mid to high temperature TE applications (400–600 °C) as their constituents are highly abundant, inexpensive, non-toxic and maintain a high stability [13]. Higher manganese silicides (HMS) are represented by $MnSi_{2-x}$, $MnSi_{1.75}$ and $MnSi_{1.8}$ compositions. They consist of a homologous series of crystallographically distinct phases referred to as the Nowtony Chimney Ladder phases. Four distinct phases of HMS have been reported with the atomic positions determined by XRD: Mn_4Si_7, $Mn_{11}Si_{19}$, $Mn_{15}Si_{26}$ and $Mn_{27}Si_{47}$ [14]. HMS are semiconductors with band gap energy from 0.4 eV to 0.7 eV [15]. They possess good TE properties and a maximum ZT 0.6 at 725 K have been reported by Gelbstein and co-workers [16].

* Corresponding authors.

http://dx.doi.org/10.1016/j.jallcom.2014.09.016
0925-8388/

Introduction of metallic inclusions may enhance the TE performance of HMS compounds. Electron and phonon collisions at the surface of the embedded particles significantly shortens their effective mean free path that may enhance the electrical properties and reduces the thermal conductivity [17]. Currently, there is not a single existing model that can describe the heat transport through composite materials containing dispersed metallic particles. Yamada et al. reported on iron and sodium added HMS samples and achieved a *ZT* of 0.31 at 800 K [18]. However, few results have been focusing on the partial substitution of Si by other elements to enhance the power factor. Luo et al. reported that substitution of Si by Al enhanced the figure of merit by 40% compared to undoped HMS samples [19]. Though, the thermal conductivity of such samples has not been reduced significantly. Similar claims were published by Ponnambalam et al. that Cr substituted $MnSi_{1.73}$ sample has raised the *ZT* about 42% as compared to undoped $MnSi_{1.73}$ [20]. Conventionally, HMS is fabricated through expensive and long term melting techniques to obtain the desired composition and crystal phases.

The goal of this work is the synthesis and detailed characterization of densely packed HMS nanocomposites (NC) containing Ytterbium (Yb), i.e. Yb–HMS composites. Yb is mainly used as a dopant of stainless steel or active laser media. Rare-earth elements, including Yb, have been observed to improve the performance of some other thermoelectric compounds [21], which is the reason for our choice of dopant for HMS. To the best of our knowledge there is no previous report about rare earth metal inclusions in HMS systems to date. In this work we have utilized ball milling (BM) and spark plasma sintering (SPS) to prepare and consolidate HMS and their Yb nanocomposites.

2. Experimental

Yb–HMS NCs were synthesized from 325 mesh silicon (Si) with 99.999% purity, manganese (Mn) powder with 99.95% purity obtained from Alfa Aesar and Yb chips with 99.99% purity from Sigma Aldrich was used. Each element was weighed under Argon, in a glove box and loaded into tungsten carbide (WC) jar and balls with hexane as dispersion media for BM. Si to Mn molar ratio was 1.73 and 0.5 wt% and 1.0 wt% Yb metal content were used for two NC samples. Planetary BM with a speed of 400 rpm was performed for 8 h. Afterwards, powder was collected and dried at room temperature in the glove box to remove the excess solvent. Subsequently, the SPS compaction was carried out by using a Dr. Sinter 2050 setup, where all the compacts were made from powders filled in a graphite die having diameter of 15 mm, using optimized SPS conditions as described in our earlier work [22]. All the samples were sintered at 950 °C for 5 min holding time at an applied pressure of 75 MPa. After sintering, the samples were polished in order to remove the graphite layer.

2.1. Characterization

HMS crystal phases were identified by X-ray diffraction (XRD) utilizing Panalytical diffractometer (operated at 45 kV and 40 A) with a Cu Kα source, wavelength 1.543 Å. Rietveld refinement of the XRD profiles was performed by the MAUD program for quantitative phase analysis, determination of crystallite sizes, and to obtain the theoretical densities of the compacted pellets (employing only the revealed crystallographic phases). Pellet densities were estimated via geometrical measurements. Morphology and composition of the samples were evaluated by performing field-emission scanning electron microscopy (FE-SEM) equipped with an Oxford energy-dispersive spectroscopy (EDS) setup. Focused ion beam (FIB) SEM was used to prepare the transmission electron microscopy (TEM) sample. HRTEM analysis was carried out by Philips TM30 TEM with an accelerating voltage of 200 keV, mapping and elemental composition analysis was performed with coupled EDS detector. SPS compacted sample was ground and particles were dispersed in ethanol which was then dropcast on the TEM grids to prepare HRTEM sample.

Thermal diffusivity was measured by a laser flash apparatus from Netzsch (LFA 457 MicroFlash) while thermal conductivity (κ) was calculated from the equation, $\kappa = \alpha\rho C_p$, where α is the thermal diffusivity, ρ is the bulk density and C_p is the specific heat of the material. The specific heat capacity was calculated by means of Netszch Proteus analysis software, comparing the samples against the standard material Netszch Pyroceram 9606. The Seebeck coefficient and electrical resistivity were measured from room temperature (RT) to 600 °C using an in house built apparatus described in details elsewhere [23]. All measurements were carried out under Ar atmosphere.

3. Results and discussion

Fig. 1 shows XRD patterns of BM samples from pure HMS and NCs. The results indicate the presence of only MnSi, Mn and Si phases and similar observations were stated also in other reports after the BM step [24,25]. It is difficult to distinguish between all the distinct crystallographic phases and these structures differ only by the *c*-axis, which is in all cases very long, compared to the *a*-axis [26]. Pure HMS BM sample phase contents were identified as 51 wt% HMS, 22 wt% MnSi, 12 wt% Si and 14 wt% Mn from Rietveld fitting data. Sadia et al. reported optimized ball milling parameters: they concluded that increase of milling time will not facilitate formation of more HMS phase [25], instead it possibly increases the metallic content of MnSi, which is detrimental for the TE performance [24]. Fig. 1(b and c) are the XRD patterns of Yb–HMS NCs: Yb peaks (ICSD # 43585) were not observed since the Yb content is close to the detection limit of the lab XRD tool. Fig. 2 displays the XRD patterns of SPS compacted sample where all major characteristic peaks of pure HMS appeared, which were in good agreement with those reported by Karpinsky and Evseev [27]. All the peaks were indexed with the tetragonal HMS with $MnSi_{1.73}$ (ICSD # 43059) and cubic MnSi (ICSD # 71830) phases. XRD results on SPSed samples are in good agreement with earlier reports [22,25,28,29]. Higher contents of Yb (more than 1.0%) resulted in inhomogeneous composites among the ones having high fraction of MnSi intermetallic phase; this is the reason why they were not used for further characterization.

Crystallite size, phase content and theoretical densities of compacted samples were obtained from the Rietveld refined curves and are reported in Table 1. All pellets are dense (more than 93%) and the crystallite size is in the range of 120–160 nm. SPS compaction has assisted for solid-state reaction to attain complete HMS phase (about 90%) phase. Furthermore, Yb–HMS NCs showed less MnSi phase and more densification as compared to pure HMS (as reported in Table 1) that is also favorable for improved TE properties.

SEM micrographs elucidated the morphology and grain size; results from BM sample, SPS compacted pure HMS and Yb–HMS NCs are displayed in Fig. 3(a–d), respectively. BM nanopowder shows inhomogeneous morphology with some agglomeration, that is attributed to the wet milling process, and particle size in the range of 50–500 nm, as shown in Fig. 3(a). Fractured surfaces of SPS compacted samples from pure HMS, 0.5% and 1% Yb–HMS NCs are presented in Fig. 3(b–d). Fractured surfaces revealed that most of the grains are below 500 nm and very little porosity was observed in compacted samples. However, we observed

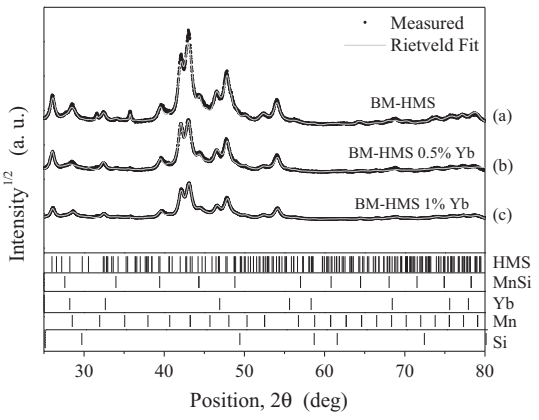

Fig. 1. XRD pattern of BM powders (a) HMS pure, (b) HMS with 0.5% Yb inclusion, (c) HMS with 1% Yb inclusion.